

Heat Transfer and Frictions in the Rectangular Divergent Channel with Ribs on One Wall

MyungSung Lee*

Evaluation Team, Gyeongnam Institute for Regional Program Evaluation, Changwon 51401, Republic of Korea

SooWhan Ahn

Department of Mechanical and System Engineering, Institute of Marine Industry, Gyeongsang National University, Tongyeong 53064, Republic of Korea

Abstract

An investigation of ribbed divergent channel was undertaken to determine the effect of rib pitch to height ratio on total friction factor and heat transfer results in the fully developed regime. The ribbed divergent rectangular channel with the channel exit hydraulic diameter (D_{ho}) to inlet channel hydraulic diameter (D_{hi}) ratio of 1.16 with wall inclination angle of 0.72 deg, at which the ratios (p/e) of 6, 10, and 14 are considered. The ribbed straight channel of $D_{ho}/D_{hi}=1.0$ were also used. The ribbed divergent wall is manufactured with a fixed rib height (e) of 10 mm and the ratio of rib spacing (p) to height 6, 10, and 14. The measurement was run with range of Reynolds numbers from 24,000 to 84,000. The comparison shows that the ratio of $p/e=6$ has the greatest thermal performance in the divergent channel under two constraints; identical mass flow rate and identical pressure drop.

Key words: divergent rectangular channel, transverse ribs, total pressure drop, heat transfer, thermal performance

1. Introduction

In general, gas turbine cooling is achieved by bleeding some relatively cool air from the compressor and using it inside the gas turbine blades to remove heat transferred into the blade from the hot mainstream. The cooling air flows through internal cooling passages inside the blade, these passages are specifically designed to maximize the heat transfer.

Many cooling techniques are in use, such as film cooling, pin-fin cooling and rib turbulated cooling. Ahn et al. [1] conducted the experimental researches on the heat transfer and friction factors in a square straight channel with one, two, and four ribbed walls. They drew the conclusion that the best heat transfer performance occurred with one ribbed wall, which had a maximum of 93% greater heat transfer performance factor than the smooth wall at $Re=7,600$.

Han et al. [2] measured the combined effects of rib angle,

rib shape, and rib pitch to height ratio on friction factors and heat transfer results. A straight parallel plate geometry along the streamwise distance was used. The experimental results showed that both the Stanton number and friction factor have a maximum value when the pitch-to-height ratio of the rib is approximately ten.

Taslim and Wadsworth [3] showed the effect of rib spacing on Nusselt number for relatively large e/D_h ratio of 0.25 in the 3.81 cm x 3.81-cm-straight square cross-sectional channel. Results for this blockage rib study indicate that variation of the average Nusselt number is not strongly dependent on the rib spacing.

As far as can be ascertained, few significant studies were found in the existing literature that deals with heat transfer in the ribbed divergent channel. However, the problem has been studied with great thoroughness in relations to the effect of divergence and convergence in the channel of developing

flow [4], and the effects of rib angle in the divergence of developed flow [5].

Wang et al. [4] investigated experimentally the local heat transfer and pressure drop characteristics of the developing turbulent flows of air in the convergent and divergent stationary ribbed square channels. And Lee et al. [5] checked out heat transfer and friction factors of fully developed turbulent flows in the rectangular divergent channel with four different parallel angled ribs. The ribbed rectangular divergent channel has the wall inclination angle of 0.72 deg at the left and right walls, corresponding to $D_{ho}/D_{hi}=1.16$.

It is thus the objective of the present study to perform the experimental investigation of the effect of the ratio of rib pitch (p) to height (e) on heat transfer and friction factors in the ribbed divergent rectangular channel with the channel exit hydraulic diameter (D_{ho}) to inlet channel hydraulic diameter (D_{hi}) ratio of 1.16, at which the ratios (p/e) of 6, 10, and 14 are considered. The straight ribbed square channel of $D_{ho}/D_{hi}=1.0$ is also considered as a comparison.

2. Experimental Apparatus

An experimental facility was constructed to test the augmentation technique. The test facility was very similar to that of Ref. [5]. Fig. 1 shows a schematic of the test rig. Air was the working fluid; constant wall heat flux was the boundary condition. The Reynolds number range of this study extended from 24,000 to 84,000; the p/e ratios varied from 6, 10, and 14; while the e/Dh ratio was 0.117. A blower located at the downstream end of the test loop forced air at room temperature through a honeycomb with a 2,500 mm long entrance section, a test section of 1,000 mm, and a 3-inch-dia and 1,400-mm-long pipe equipped with a multipoint average Pitot tube to measure the fluid flow rate.

The rectangular divergent channel has the cross section of 75 x 100 mm² at the inlet and 100 x 100 mm² at the outlet, as shown in Fig. 2. This geometry makes the rectangular

divergent channel have an angle of 0.72 deg along the streamwise direction in the test section. Each of left and right heating walls is subdivided into 10 sub-sequential regions, each comprising 1 copper plate of 100 mm x 100 mm x 2 mm(t). Regions are separated by rubber gaskets to

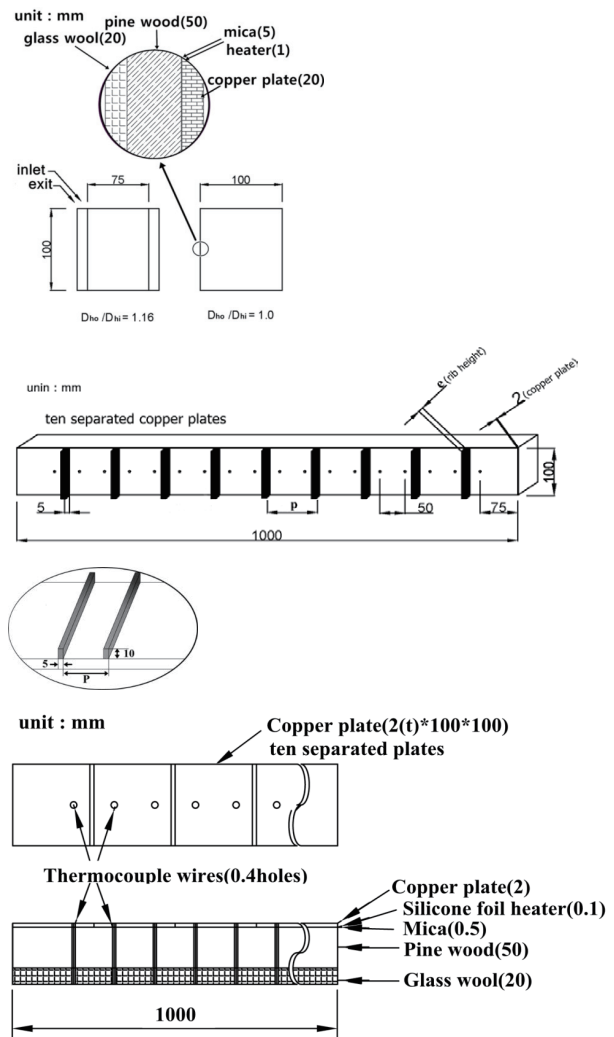


Fig. 2. Details of test section

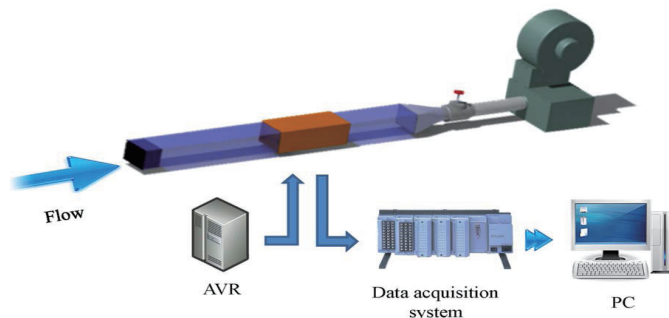


Fig. 1. Schematic of experimental facility

inhibit thermal conduction between the copper plates. The transverse ribs placed in parallel are attached on the left wall only. The other opposite walls (top and bottom) are left smooth and insulated.

The 0.1 mm-thick silicone heaters are glued to the back of each wall (left and right). The power input can be varied by controlling a single phase transformer and measured by the voltage applied to the heater. Each of plates is instrumented with T-type copper-constantan thermocouples. The thermocouples are buried inside a 0.4-mm-dia holes drilled on the plate and held in place by using an epoxy resin.

The test section is installed in a 50-mm-thick pine wood housing. Further insulation is provided by encapsulating the entire test section in a thick layer of glass wool. The maximum wall temperature was less than about 85°C. 9 pressure taps are set up at the same interval along the top smooth wall center. Static pressures are measured by an inclined manometer or a digital manometer with a resolution up to 0.01 mm H₂O at the static pressure of 19.99 mm H₂O.

3. Experimental Accuracy

In all tests, in order to reduce the thermocouple inaccuracy which strongly affects the calculated heat transfer coefficient, the room air temperature was maintained between 21 and 27°C and the temperature difference between the heated wall and fluid was maintained between 13 and 22°C.

The inlet air temperatures were measured by thermocouples checked by a thermometer with resolution of 0.1°C. The bulk temperature of exiting air was measured by five thermocouples distributed at different vertical locations of the outlet cross section. The longitudinal distribution of the fluid bulk mean temperature was represented as a straight line connecting the measured mean values at inlet and exit. In order to reduce the thermocouple inaccuracy, which strongly affects the calculated heat transfer coefficient, the temperature rise of room air was maintained at the unvaried condition.

The heater affixed to ten copper plates provides constant heat flux. Adjusting the voltage across the heater changes the steady state temperature measured on each copper plate. Here, the heat flux loss, q_l occurring due to conduction through the test section to the air in the room was calculated as follows:

$$q_l = \frac{T_w - T_\infty}{\frac{\Delta y_1}{k_1} + \frac{\Delta y_2}{k_2} + \frac{\Delta y_3}{k_3} + \frac{1}{h_1}} \quad (1)$$

Where T_∞ is the ambient temperature, Δy_1 and k_1 are the thickness and conductivity of mica (0.71 W/m°C), Δy_2 and

k_2 are the thickness and conductivity of pine wood (0.112 W/m°C), Δy_3 and k_3 are the thickness and conductivity of glass wool (0.038 W/m°C), and h_1 is the ambient natural convective heat transfer coefficient (6.5 W/m²°C). A low conductivity material is placed inside the test section to inhibit heat transfer within the test section.

The maximum heat flux loss was within 5.8%. The net heat transfer rate was defined as:

$$Q - Q_{loss} = \dot{m} c_p (T_{bo} - T_{bi}) \quad (2)$$

Where \dot{m} is the air mass flow rate. T_{bi} and T_{bo} are the bulk mean air temperatures at the inlet and outlet of test section, respectively. The thermocouples were calibrated in advance and their accuracy is estimated to be about 0.2°C.

The total friction factor (f_T) considering the dynamic pressure drop (ΔP_T) is defined as:

$$\Delta P_T = P_i - P_o + \frac{1}{2} \rho u_{bi}^2 - \frac{1}{2} \rho u_{bo}^2 \quad (3)$$

$$f_T = \frac{D_h}{2 \rho u_b^2} |\Delta P_T / L| \quad (4)$$

Where P_i and P_o are the static pressure drops at the inlet and outlet. The average hydraulic diameter of test section, D_h is $(D_{hi} + D_{ho})/2$. And Reynolds number is obtained as follows:

$$Re = \frac{u_b D_h}{\nu} \quad (5)$$

Where D_h is 93.3 mm and u_b is the air bulk velocity ranging from 4 m/s to 14 m/s at the mid test section, corresponding to 0.035 m³/s to 0.1225 m³/s. The local heat transfer coefficient, h is defined as:

$$h_x = \frac{(Q - Q_{loss})}{A(T_{wx} - T_{bx})} \quad (6)$$

Where the heat transfer area, A is based on the projected heat transfer area. The channel average Nusselt number, Nu is defined as:

$$Nu = \frac{\bar{h} D_h}{k} \quad (7)$$

Where \bar{h} is the channel average heat transfer coefficient and k is the thermal conductivity of air. An uncertainty evaluation was run as suggested by Kline and McClintock [6]. The maximum uncertainty in the average Nusselt number was estimated to be less than 11% and that for the friction factor less than 12%. The two constraints for thermal performance comparison are adopted: identical mass flow rate and identical pressure drop. Based on the constant property assumption, the formulations of the two constraints are given as follows:

a) Identical mass flow rate:

Mass flow rate is given by

$$(\rho u_b \frac{D_h}{4} Pe)^* = (\rho u_b \frac{D_h}{4} Pe) \quad (8)$$

Where Pe is the average perimeter of test section

$$Re^* = Re \left(\frac{A_c}{A_c^*} \right) \left(\frac{D_h}{D_h^*} \right) \quad (9)$$

Where A_c is the average cross sectional area of test section.

b) Identical pressure drop

Pressure drops can be defined as

$$\left(\frac{1}{2} f \rho u_b^2 \frac{Pe}{L} \frac{L}{A_c} \right)^* = \left(\frac{1}{2} f \rho u_b^2 \frac{Pe}{L} \frac{L}{A_c} \right) \quad (10)$$

Where L is the length of test section.

$$Re^* = [(f Re^2 / D_h^3) / (f / D_h^3)^*]^{1/2} \quad (11)$$

Where the superscript $*$ shows the compared channel and the quantity without $*$ shows the reference channel (smooth straight cross section channel). The ratio of the heat transfer between the compared channel and reference channel is formulated as follows:

$$\frac{H^*}{H} = \frac{[Nu(Re)]^*}{Nu(Re)} \quad (12)$$

4. Results and Discussion

Figure 3 represents the static pressure drops along the streamwise distance in the ribbed divergent channel of $D_{ho}/D_{hi}=1.16$ as a function of the ratio of rib pitch (p) to height (e). The magnitude of static pressure drops in terms of the ratio of p/e can be seen in the order of $p/e = 6, 14$, and 10 .

This is the contrary to the experimental results [2] for the ribbed straight cross section channel along the streamwise distance that the maximum static pressure drop occurs at the pitch-to-rib height ratio (p/e) of 10 , at which the flow does reattach close to the succeeding rib.

This discrepancy is attributed to the fact that the deceleration flows along the streamwise distance in the ribbed divergent channel make additional vortices along the streamwise distance except those behind the ribs. Furthermore, research would be needed to elucidate the critical ratio of p/e in the ribbed divergent channel, corresponding to maximum static pressure drops. The total pressure drops (ΔP_T) defined as Eq. (3) in the ribbed divergent channel of $D_{ho}/D_{hi}=1.16$ and the ribbed straight cross section channels of $D_{ho}/D_{hi}=1.0$ with identical cross-section area are shown in Fig. 4. Contrary to the static pressure drops in Fig. 3 in the ribbed divergent channels, the

pitch-to-rib height ratio (p/e) of 10 produced the greatest values in the total pressure drops. It would be due to the definition of total pressure drops in Eq. (3). The total pressure drops in the ribbed straight cross section channel along the streamwise distance have negative ones because the blower

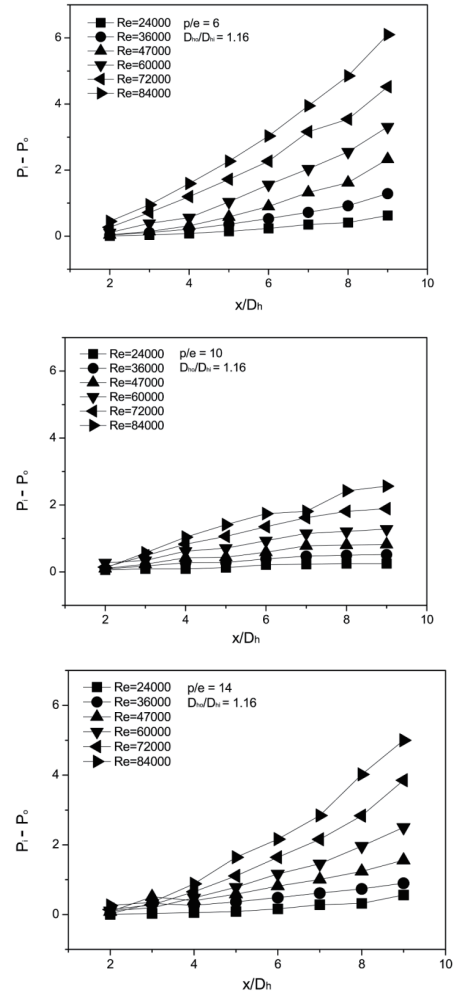


Fig. 3. Static pressure drops

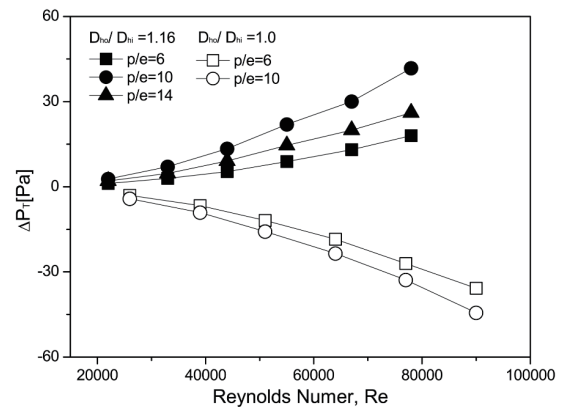


Fig. 4. Total pressure drop

forcing air is located at the downstream end of the test loop and no dynamic pressure drops occur.

Total pressure drops in the divergent channel increase because the total pressure drops are subject to the combination of static pressure drop ($P_1 - P_0$) and dynamic pressure drop ($\rho u_{b1}^2 - \rho u_{b02}$). The Reynolds number dependences of total friction factors for various ratios of p/e in the ribbed channels of $D_{ho}/D_{hi}=1.16$ and 1.0 are shown in Fig. 5.

Contrary to our previous work [7] that the inclined wall channel would have greater total friction factors than those of straight cross section channel, the total friction factors in the ribbed divergent channel of $D_{ho}/D_{hi}=1.16$ were somewhat lower than in the straight ribbed channel of $D_{ho}/D_{hi}=1.0$. It would be due to the fact that the slight divergent channel wall with 0.72-deg-inclination generates very low static pressure drops as shown in Fig. 3.

The subscript ss was predicted by Blasius's equation for the smooth circular tube [8]. For a comparison, Taslim and Wadsworth's experimental results [3] for the ribbed straight cross section channels were included.

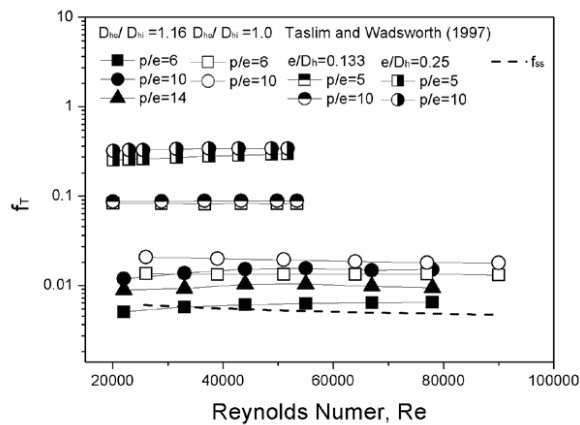


Fig. 5. Total friction factors

Much greater friction factors were observed in Taslim and Wadsworth's experimental results [3] rather than the present work. It might be attributed to the fact that Taslim and Wadsworth used transverse ribs of $e/D_h=0.133$ and 0.25 on two opposite walls as opposed to $e/D_h=0.117$ on one wall only.

Figure 6 shows the channel average Nusselt numbers against the ratio of p/e on the ordinate with Reynolds number on the abscissa. Contrary to the total friction factors (f_t) in Fig. 5, the Nusselt numbers in $D_{ho}/D_{hi}=1.16$ were greater than in $D_{ho}/D_{hi}=1.0$. It is proved that the ribbed divergent channel of $D_{ho}/D_{hi}=1.16$ is advantageous over the ribbed straight channel of $D_{ho}/D_{hi}=1.0$ in the thermal design.

For a comparison, Taslim and Wadsworth's result for the straight ribbed square channel is included. Taslim and Wadsworth's result is much higher than in the present study. This is expected to have resulted from the higher friction factor, which makes the greater turbulent mixing close to the heat transfer surface [2]. The subscript ss was proposed by Dittus and Boelter's equation for the smooth circular tube [9].

The comparisons of the channel average thermal

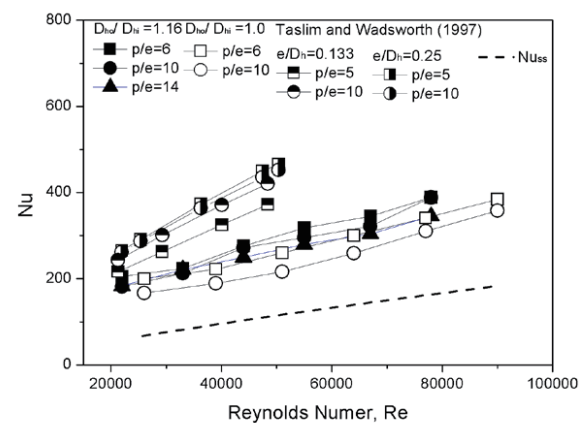
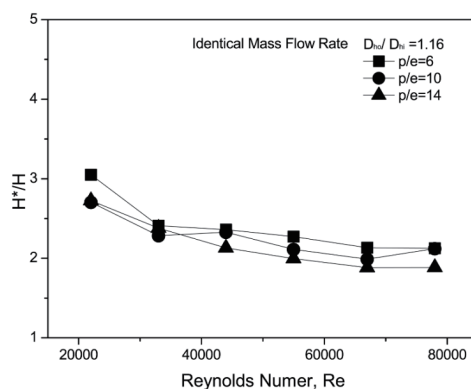
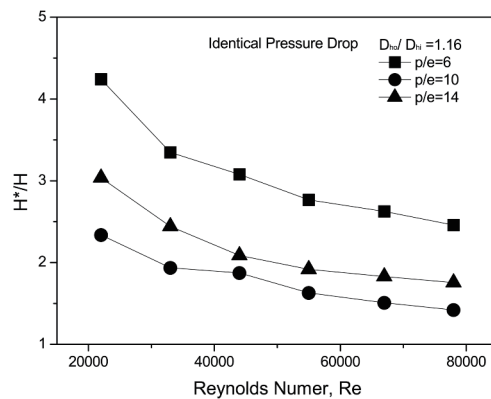


Fig. 6. Channel average Nusselt numbers



(a) Identical mass flow rate



(b) Identical pressure drop

Fig. 7. Thermal performances

performances for the ribbed divergent channels shown in Fig. 7, where the ratios of the heat transfer in the ribbed divergent channel to in the smooth circular tube. From Fig. 7(a), it can be seen that in the identical mass flow rate, the heat transfer enhancement is about 1.9 to 2.2 times at Reynolds number of 60,000, compared with the smooth circular tube.

Figure 7(b) shows that in the identical pressure drop, the heat transfer enhancement is 1.6 to 2.8 times at Reynolds number of 60,000, compared with the smooth circular tube. The ratio of $p/e=6$ has the greatest thermal performance in the divergent channel under two constraints; identical mass flow rate and identical pressure drop.

The preceding comparison indicates that the ribbed divergent channel has the higher thermal performance than that of the smooth circular tube.

5. Conclusions

1) The total friction factors in the ribbed divergent channel of $D_{ho}/D_{hi}=1.16$ were somewhat lower than in the straight ribbed channel of $D_{ho}/D_{hi}=1.0$

2) The ribbed divergent channel of $D_{ho}/D_{hi}=1.16$ is advantageous over the ribbed straight channel of $D_{ho}/D_{hi}=1.0$ in the thermal design.

3) The ratio of $p/e=6$ has the greatest thermal performance in the divergent channel under two constraints; identical mass flow rate and identical pressure drop.

Acknowledgement

This Work was Supported by Development Fund Foundation, Gyeongsang National University, 2015.

References

- [1] Ahn, S. W., Kang, H. K., Bae, S. T. and Lee, D. H., "Heat Transfer and Friction Factor in a Square Channel with One, Two, and Four Ribbed Walls", *ASME Journal of Turbomachinery*, Vol. 130, 2008, pp. 034501-5.
- [2] Han, J. C., Glicksman, L. R. and Rohsenow, W. M., "An Investigation of Heat Transfer and Friction for Rib-roughened Surfaces", *International Journal of Heat and Mass Transfer*, Vol. 21, 1978, pp. 1143-1156.
- [3] Taslim, M. E. and Wadsworth, C. M., "An Experimental Investigation of the Rib Surface-Averaged Heat Transfer Coefficient in a Rib-roughened Square Passage", *ASME Journal of Turbomachinery*, Vol. 119, 1997, pp. 381-389.
- [4] Wang, B., Tao, W. Q., Wang, Q. W. and Wong, T. T., "Experimental Study of Developing Turbulent Flow and Heat Transfer in Ribbed Convergent/divergent Square Ducts", *International Journal of Heat and Fluid Flow*, Vol. 22, 2001, pp. 603-613.
- [5] Lee, M. S., Jeong, S. S., Ahn, S. W. and Han, J. C., "Effects of Angled Ribs on Turbulent Heat Transfer and Friction Factor in a Rectangular Divergent Channel", *International Journal of Thermal Science*, Vol. 84, 2014, pp. 1-8.
- [6] Kline S. J. and McClintock, F. A., "Describing Uncertainty in a Single Sample Experiment", *Mechanical Engineering*, Vol. 75, 1953, pp. 3-8.
- [7] Lee, M. S. and Ahn, S. W., "Heat Transfer and Friction Factors in the Ribbed Square Convergent and Divergent Channels", *Heat and Mass Transfer*, Vol. 52, 2016, pp. 1109-1116.
- [8] Incropera, F. P. and Dewitt, D. P., *Fundamental of Heat and Mass Transfer*, 4th ed., John Willy and Sons, Inc., 1996, pp. 424.
- [9] Holman, J. P., *Heat Transfer*, 8th ed., McGraw-Hill, Inc., New York, 1997, pp. 218-282.